Journal of Colloid and Interface Science 326 (2008) 66–71

Contents lists available at ScienceDirect

Journal of Colloid and Interface Science

www.elsevier.com/locate/jcis

Surfactant dependent morphology of polymeric capsules of perfluorooctyl bromide: Influence of polymer adsorption at the dichloromethane–water interface

Emilia Pisani [a,b], Elias Fattal [a,b], Juliane Paris [a,b], Catherine Ringard [a,b], Véronique Rosilio [a,b], Nicolas Tsapis [a,b,*]

[a] Univ Paris Sud, UMR CNRS 8612, Faculté de Pharmacie, Châtenay-Malabry, France
[b] CNRS, UMR 8612, Faculté de Pharmacie, Châtenay-Malabry, France

ARTICLE INFO

Article history:
Received 9 June 2008
Accepted 8 July 2008
Available online 16 July 2008

Keywords:
Polymeric capsules
Perfluorooctyl bromide
Encapsulation
Surfactant
Morphology

ABSTRACT

In a strategy to develop more stable ultrasound contrast agents (UCAs), we have designed a process to obtain nano/microcapsules with a single core of liquid perfluorocarbon within a biodegradable polymeric shell of homogeneous thickness. During the optimization of perfluorooctyl bromide (PFOB) encapsulation by solvent emulsion-evaporation, a marked influence of surfactants has been observed. While sodium cholate leads to spherical capsules of homogeneous thickness, sodium taurocholate induces to the formation of "acorn"-particles with one hemisphere of PFOB and another one of PLGA, and polyvinyl alcohol is responsible for the coexistence of both morphologies. Whereas the theoretical model proposed by Torza and Mason [J. Colloid Interface Sci. 33 (1970) 67] fails to predict the observed morphologies, microscopic observations of the evaporation and interfacial tension measurements provide an insight into the mechanism of formation of these structures. Most probably, there is a competition between PLGA and the surfactant stabilizing the emulsion at the dichloromethane–water interface. If PLGA is able to adsorb at the interface, the core–shell morphology is obtained, otherwise the acorn morphology is preferentially formed. When the surfactant rearrangement at the interface is long (>30 min), a coexistence of morphologies can be obtained.

1. Introduction

Efficient ultrasound contrast agents (UCAs) requires controlled acoustic properties to lead to a more widespread clinical use [1,2]. In a strategy to develop more efficient UCAs, we have designed a process to obtain nano/microcapsules with a single core of liquid perfluorooctyl bromide (PFOB) within a biodegradable [3] and biocompatible [4] polymeric shell of poly(lactide-co-glycolide) (PLGA) of homogeneous thickness [5,6]. The polymer shell should improve the stability of the capsules as compared to UCAs stabilized by a monomolecular layer, while the acoustic impedance of PFOB should insure their echogenicity [7]. Engineering core–shell capsules is not as straight forward as one might imagine [8,9]. Pioneer work by Torza and Mason [10] established that the engulfing mechanism involves two competitive processes: penetration and spreading. Briefly, if droplets of immiscible liquids (phases 1 and 3) are brought in contact in a third mutually immiscible liquid (phase 2), the final equilibrium morphology can be rationalized by analyzing the various interfacial tensions between the phases (γ_{12}, γ_{23}, and γ_{13}). By defining the spreading coefficients S_i for each phase as

$$S_i = \gamma_{jk} - (\gamma_{ij} + \gamma_{ik}) \tag{1}$$

and designating phase 1 to be that for which $\gamma_{12} > \gamma_{23}$, then $S_1 < 0$. It then follows that there are only three possible combinations of S_i,

$$S_1 < 0; \quad S_2 < 0; \quad S_3 > 0, \tag{2}$$

$$S_1 < 0; \quad S_2 < 0; \quad S_3 < 0, \tag{3}$$

$$S_1 < 0; \quad S_2 > 0; \quad S_3 < 0. \tag{4}$$

When the conditions in Eq. (2) are satisfied the particles adopt a core–shell morphology with phase 1 appearing as the core within a shell of phase 3. When Eq. (3) is satisfied, "acorn"-shaped particles are formed, and when Eq. (4) is satisfied two separate droplets are preserved (Fig. 1).

An alternative model based on the analysis of the thermodynamics of two-stage particle formation has been developed by Sundberg et al. [8,11]. In their approach, the system was considered in terms of the free energy changes at the interfaces of a three-phase system (i.e., in their case polymers 1 and 2 and water) based on $G = \sum \gamma_{ij} A_{ij}$, where G is the Gibbs free energy. According to this analysis, each specific morphological configuration has a

* Corresponding author at: Université Paris Sud, UMR CNRS 8612, Faculté de Pharmacie, 5 Rue Jean-Baptiste Clément, 92296 Châtenay-Malabry, France. Fax: +33 146619334.
E-mail address: nicolas.tsapis@u-psud.fr (N. Tsapis).

0021-9797/$ – see front matter
doi:10.1016/j.jcis.2008.07.013

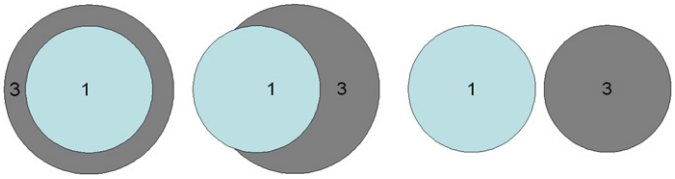

Fig. 1. Expected morphologies when Eq. (2) is satisfied (left), Eq. (3) is satisfied (middle) and Eq. (4) is satisfied (right).

different value for G, and the configuration with the minimal free energy is thermodynamically favored [8]. Several apparently different morphologies (hemispherical, sandwich, multiple lobes) have been found to coexist at the same time within a single emulsion, suggesting that they may be merely different states of phase separation and not thermodynamically stable, unique morphologies. The results of Sundberg et al. strongly suggest that equilibrium morphologies are not always obtained [8,11]. This is not the case in the results of Torza and Mason [10] since they worked with incompatible pairs of low molecular weight compounds that diffuse readily. The replacement of one of these compounds with a high molecular weight polymer brings the issue of diffusive restrictions, such as polymer chain mobility, into consideration. Sundberg et al. [8] have found that it is possible to achieve non-equilibrium morphologies, especially when the solvent is removed rapidly, even when one of the organic components is a low-viscosity liquid. They have designated such morphologies as "rate-limited morphologies" by contrast with equilibrium morphologies and have suggested that an infinite number of states of phase separation may exist depending on the speed of the process (e.g. solvent evaporation).

During the optimization of perfluorooctyl bromide (PFOB) encapsulation into PLGA capsules by solvent emulsion-evaporation, the influence of different preparation parameters on final microcapsule morphologies has been studied in detail. In particular, we have studied the influence of the evaporation speed and the polymer concentration in the organic phase among other preparation parameters such as the volume of the different phases or the surfactant concentration. A marked influence of the surfactants used during the emulsification step of the process has been observed using different types of microscopy. Results have been rationalized using the models presented above and by measuring interfacial tensions between the different interfaces.

2. Experimental part

2.1. Materials

Poly(lactide-co-glycolide) Resomer RG502 was provided by Boehringer–Ingelheim (Germany). Polyvinyl alcohol (MW 30 000–70 000, 89% hydrolyzed), sodium cholate (SC), sodium taurocholate (TC) and Nile Red were provided by Sigma–Aldrich. Perfluorooctyl bromide (PFOB) from Fluorochem (UK). Dichloromethane RPE-ACS 99.5% was obtained from Carlo Erba Reactifs (France). The ultrapure water ($\gamma = 72.4$ mN/m at 22 °C) was produced by a Millipore Synergy 185 apparatus coupled with a RiOs5^{TM} (Millipore, France), with a resistivity of 18.2 MΩ cm.

2.2. Methods

Optical and fluorescence microscopy were achieved as follows: Samples suspension were placed between glass slides and observed with a Leitz Diaplan microscope equipped with a Coolsnap ES camera (Roper Scientific). Fluorescent samples dyed with Nile Red were excited at 543 nm and observed at 560 nm (long-pass filter).

Confocal microscopy was performed with a Zeiss LSM-510 microscope equipped with a 1 mW Helium Neon laser, using a Plan Apochromat 63X objective (NA 1.40, oil immersion). Red fluorescence was observed with a long-pass 560 nm emission filter under 543 nm laser illumination. The pinhole diameter was set at 71 µm. Stacks of images were collected every 0.42 µm along the z-axis.

Scanning Electron Microscopy (SEM) was performed using a LEO 1530 (LEO Electron Microscopy Inc, Thornwood, NY) operating between 1 and 3 kV with a filament current of about 0.5 mA. Sample suspensions were deposited on carbon conductive double-sided tape (Euromedex, France) and dried at room temperature. They were coated with a palladium–platinum layer of about 4 nm using a Cressington sputter-coater 208HR with a rotary-planetary-tilt stage, equipped with a MTM-20 thickness controller. Before imaging, particles were washed either by centrifugation or dialysis to remove the excess of surfactant that reduces the quality of images.

Transmission Electron Microscopy was performed using a Philips EM208 operating at 80 kV. Suspensions of nanocapsules were deposited on copper grids covered with a formwar film (400-mesh) for 2 min. The excess solution was blotted off using filter paper and grids were air-dried before observation. Images were acquired using a high-resolution camera Advantage HR3/12GO4 (AMT-Hamamatsu).

Interfacial tension measurements were performed by the pendant drop method, using the Drop Shape Analysis System DSA 100 (Krüss, Germany). PFOB and dichloromethane containing or not PLGA (at 25 mg/mL) and/or PFOB drops were formed into the aqueous solution, with or without surfactant. The interfacial tension values were determined from at least ten independently formed drops. The temperature of experiments was 20 ± 1 °C. The experimental uncertainty was estimated to be lower than 0.2 mN/m.

2.3. Sample preparation

PLGA was dissolved into 4 mL dichloromethane along with 60 µL PFOB and placed in a thermostated bath maintained at 20 °C to ensure full miscibility of PFOB with dichloromethane at this concentration. The organic solution was then emulsified into 20 mL of surfactant (PVA 0.005% to 2% (w/w) or SC 1.5% (w/w) or TC 1.5% (w/w)) aqueous solution using an Ultra-turrax T25 (IKA) operating with a SN25-10G dispersing tool at a velocity of 8000 RPM. Emulsification was performed in a 50 mL beaker placed over ice for 2 min. Dichloromethane was then evaporated by magnetic stirring for about 3 h at 300 RPM in a thermostated bath (20 °C) or in a rotary evaporator under reduced pressure for about 1 h at 700 RPM (room temperature). For fluorescent or confocal microscopy, Nile Red was added to the organic solution prior to emulsification. Typically, about 100 mL of a concentrated Nile Red solution (0.057 mg/mL in dichloromethane) were added. To further decrease the capsule size and obtain nanocapsules, a pre-emulsion was prepared by mixing the organic and aqueous phases by Ultra-turrax at 8000 RPM for 30 s. This pre-emulsion was then sonicated at 300 W for another minute using a Vibra cell sonicator (Bioblock Scientific, France). The following steps of the process are the same as described for microcapsules. Fresh capsules were frozen at −20 °C after addition of PVA (final concentration 0.2% (w/v)) used as a cryoprotectant [12]. Samples were then freeze-dried for 24 to 48 h using a LYOVAC GT2.

3. Results and discussion

The method used to obtain nano/microcapsules composed of a solid polymeric shell encapsulating a liquid perfluorooctyl bromide (PFOB) core is derived from the technique described by Loxley and Vincent [13]. It is a modification of the commonly used emulsion-evaporation process. The organic phase is a mixture of PLGA, dichloromethane, a low-boiling good solvent for PLGA,

and PFOB, a high-boiling, very poor solvent for PLGA. Enough dichloromethane is present to ensure that PLGA is completely dissolved and that the liquid PFOB is fully miscible. The organic phase is then emulsified in an aqueous solution of surfactant and the low-boiling solvent is evaporated. At the beginning of the evaporation process there is only one interface in the system, the dichloromethane (including PLGA/PFOB)–water (containing a surfactant) interface. Evaporation allows gradual removing of the dichloromethane from the emulsion droplets by diffusion through the aqueous solution. Since PFOB is very poorly miscible in dichloromethane, the droplet composition reaches quickly the binodal boundary and PFOB phase-separates as small droplets within the emulsion globules of polymer–dichloromethane. At this stage, two interfaces are present: the dichloromethane (PLGA)–water interface and the dichloromethane (PLGA)–PFOB interface. When wetting conditions are correct, the polymer–dichloromethane globule fully engulfs the PFOB droplet. Further solvent removal causes the polymer to precipitate at the interface, forming a solid shell as already observed with other polymers [13]. According to Torza and Mason [10], if the polymer does not spread in a continuous monolayer at the dichloromethane–water (surfactant) interface, other morphologies than spherical core–shell capsules can be observed such as "corn" morphologies or separated droplets.

In our strategy to encapsulate PFOB, polyvinyl alcohol (PVA) was the first surfactant evaluated for capsules formulation since it is the most common emulsion stabilizer used in the pharmaceutical field to prepare micro and nanosystems [14,15].

Bright field optical microscopy shows the coexistence of spherical capsules with "acorn" particles (Fig. 2, left) consisting of a liquid hemispherical PFOB droplet and a solid PLGA hemisphere. In confocal microscopy images, regular capsules appear with PLGA dyed in red whereas PFOB is invisible, as well as half-particles corresponding to the polymeric hemisphere of an "acorn" (Fig. 2, middle). The combination of these observations leads to the conclusion that the invisible hemisphere in confocal microscopy images is liquid PFOB. In a standard suspension of capsules (0.1 g of PLGA and 60 µL of PFOB dissolved into 4 mL dichloromethane, emulsified into 20 mL of 0.5% PVA (w/v) aqueous solution), the "acorn" morphologies represent 30 to 40% of the objects in suspension in number. TEM images confirm that the balance between core–shell and "acorn" morphologies persists for capsules with diameters smaller than one micron (Fig. 2, right). This result is in agreement with Torza and Mason's theory in which the criteria of balance configuration do not include drop dimension, as well as with the thermodynamic analysis of Sundberg et al. which is independent of particle size [8]. After freeze-drying, optical microscopy and SEM images of suspensions reveal that the core–shell morphologies are preserved, whereas the "acorn" morphologies have disappeared leaving only PLGA hemispheres (Fig. 3). This indicates that PFOB has probably evaporated from the acorns during the freeze-drying process due to its low vapor pressure (1866 Pa, at 37 °C) [16]. Previous work has shown that when core–shell capsules are freeze-dried, PFOB remains encapsulated [5].

In a strategy to obtain 100% core–shell capsules in the suspension, several preparation parameters were varied in the system prepared with PVA 0.5%. Many parameters were found to have no impact on the final balance between core–shell and "acorn" morphologies. For example, the percentage of "acorns" remains close to 30–40% in number even if, in a standard preparation, (i) the volume of PFOB varies from 20 to 60 µL, (ii) the aqueous phase volume is doubled for the same PVA concentration, or (iii) the dichloromethane volume is doubled for the same PFOB/PLGA concentration. Neither the variation of the PVA concentration in the aqueous phase (between 0.005 and 2% (w/v)), nor the molecular weight of this polymeric surfactant induces a modification of the percentage of "acorns." By contrast, the PLGA concentration in the

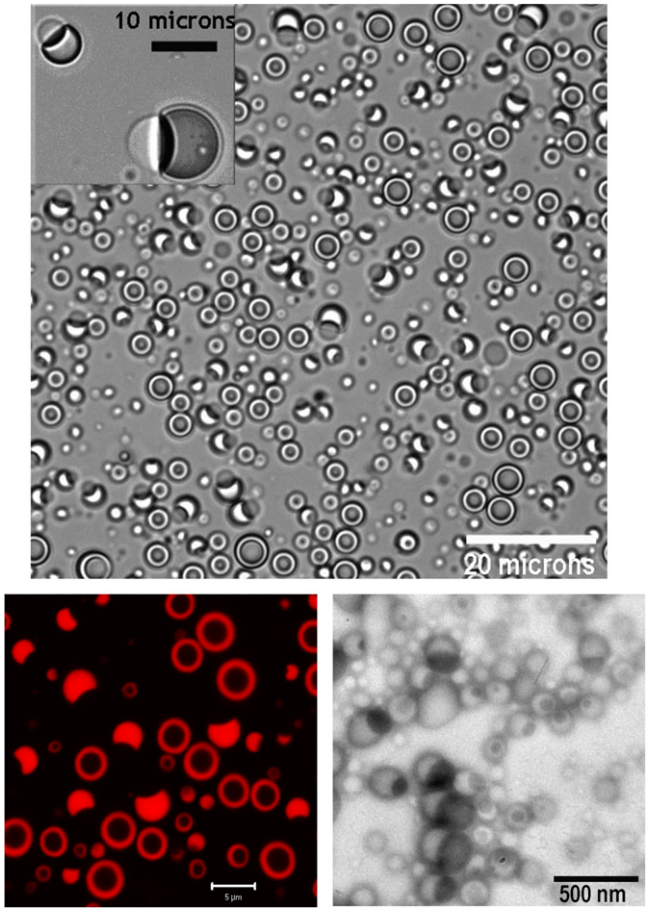

Fig. 2. Typical images of capsules suspensions obtained using PVA 0.5% (w/v) as a surfactant, observed by optical microscopy (top), confocal microscopy (bottom-left) and TEM (bottom-right). Independently of the emulsification energy applied, a coexistence of core–shell and "acorn" morphologies can be observed. The inset presents an example of the "acorn"-shaped morphology: the dark hemisphere is the polymeric fraction, while the bright hemisphere is PFOB. Scale bars represent 20 µm (top), 5 µm (bottom-left) and 500 nm (bottom-right).

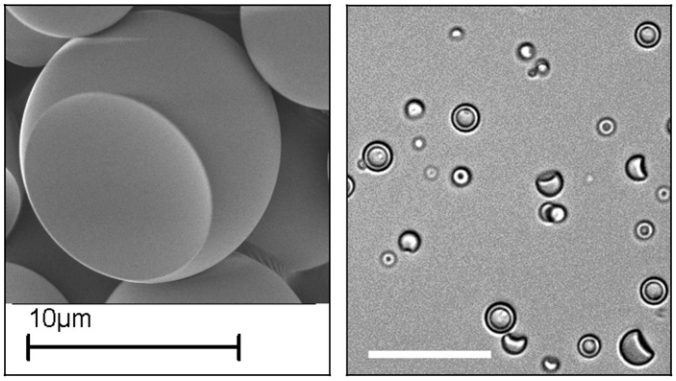

Fig. 3. SEM image of a typical "acorn" particle after freeze-drying. PFOB has evaporated and the remaining polymeric hemisphere can be observed (left). Optical microscopy image of a suspension of particles after freeze-drying (right): capsules coexist along with polymeric hemispheres (scale bar = 20 µm).

organic phase seems to be an important parameter to affect the final proportion of core–shell to "acorn" morphology: when it varies from 2.5 to 125 mg/mL, the percentage of "acorns" decreases from 73 to 20%. By increasing PLGA concentration, the organic phase viscosity increases, which demonstrate that the development of the final morphology involves the mobility or diffusion of the different chemical species, which is related to the viscosity. The

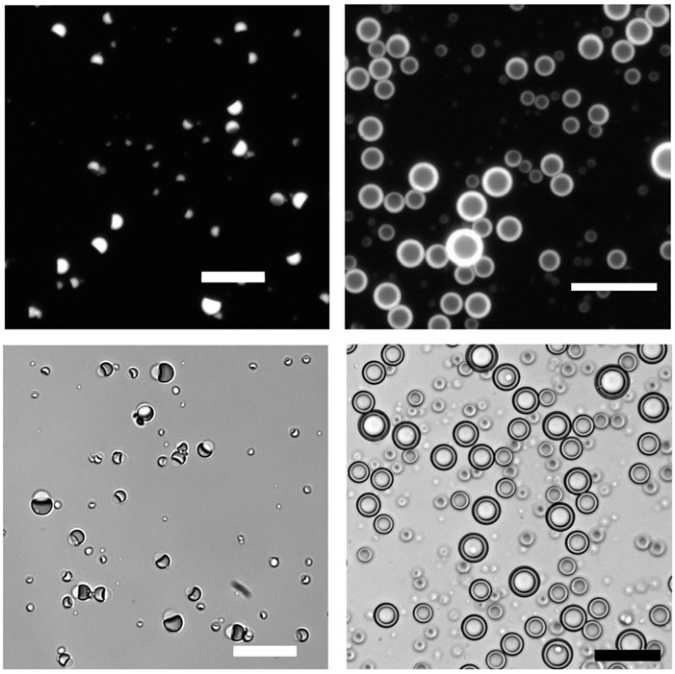

Fig. 4. Images of "acorns" obtained with TC 1.5% (left) and core–shell capsules obtained with SC 1.5% (right) observed with fluorescent microscopy (top) and bright field microscopy (bottom). Scale bars represent 20 µm in all images.

more viscous the organic phase, the more capsules can be observed.

The speed of solvent evaporation also seems to be a relevant parameter affecting the balance between morphologies. If the solvent is evaporated under reduced pressure at room temperature, the percentage of "acorns" increases from 30 to 80%, in agreement with Sundberg's results [8]. The substitution of dichloromethane (interfacial tension with water (20 °C) = 32.8 mN/m, boiling point 40 °C) by a higher boiling point solvent chloroform (interfacial tension with water (20 °C) = 28.3 mN/m, boiling point 62 °C) [17] leads to an increase in "acorn" structures (around 58% in number). Although this result is apparently in contradiction with the previous one, it is not surprising since the change of solvent also leads to a change of the interfacial tensions. Despite all the modifications performed, it should be noted that none of them allowed to totally shift the balance and to obtain only one of the possible morphologies.

In addition to PVA, several other surfactants were reviewed, but only sodium taurocholate and sodium cholate were able to utterly shift the balance to obtain only one of the two possible morphologies. Loxley and Vincent have shown that small ionic surfactants are unsuitable emulsifiers for forming core–shell capsules, as they reduce the dichloromethane–water interfacial tension more than non-ionic surfactants and yield "acorns." Indeed, using a sodium taurocholate (TC) solution at 1.5% (w/v), we obtain only the "acorn" morphology (Fig. 4, left). However, using sodium cholate, a smaller ionic surfactant, at 1.5% (w/v) in water, only core–shell capsules were observed after solvent evaporation (Fig. 4, right).

Since evaporation has some impact on the final morphology balance, we have investigated the different morphologies formation during the solvent evaporation process. After emulsification, the emulsion was collected every 15 min and observed with bright field and fluorescence microscopy. During the first hour of evaporation, no differences could be observed between emulsions prepared with SC, PVA or TC. At the end of the first hour of evaporation, independently of the surfactant used, a PFOB droplet is visible within the emulsion globules. Between the first and the second hour of evaporation, the PFOB droplet volume increases

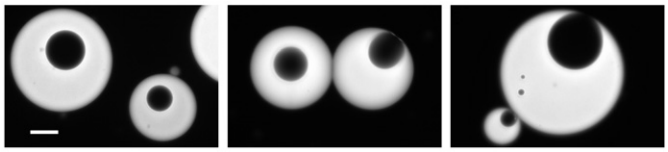

Fig. 5. Fluorescent images of emulsion globules after 2 h of evaporation (left: SC, middle: PVA, right: TC). The position of the PFOB droplet (dark) within the globule is characteristic of the surfactant used. The scale bar represents 20 µm.

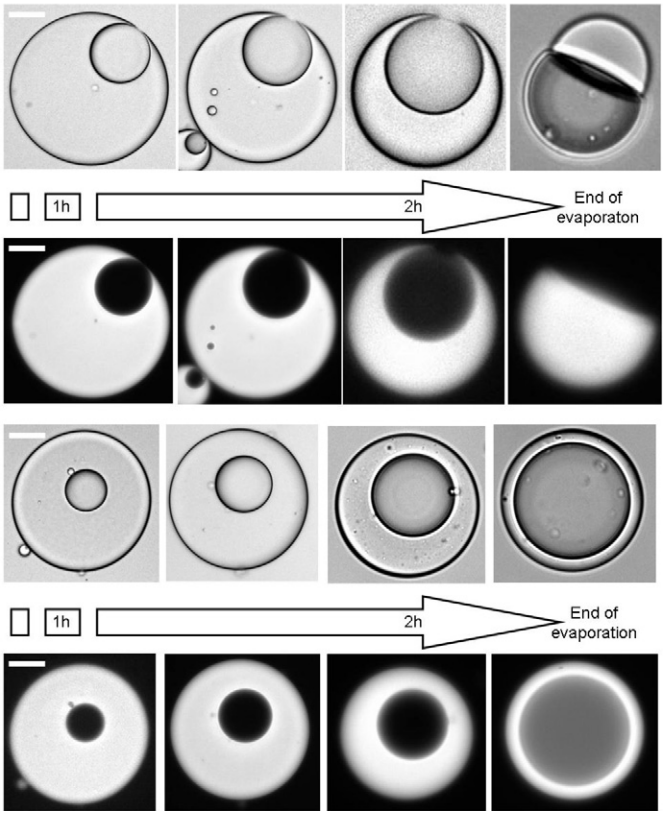

Fig. 6. Bright field and fluorescence images of the different steps of solvent evaporation for TC (top) or SC (bottom). The position of the PFOB droplet after one hour of evaporation determines the final morphology of the particle. Scale bars represent 20 µm.

but the droplet position within the globules differs for the different surfactants. On one hand, in the SC emulsions, PFOB droplets are central in all the globules (Fig. 5, left). On the other hand, in the TC emulsions, PFOB droplets are located close to the globule interface with the aqueous solution (Fig. 5, right). Finally, in the PVA emulsion, about 30–40% of PFOB droplets are situated close to the globules interface with the aqueous solution, whereas the remaining globules contain well centered PFOB droplets (Fig. 5, middle). Then, as shown in Fig. 6 top and bottom, the position of the PFOB droplet within the emulsion globule determines the final morphology obtained once the evaporation is completed. These observations, however, do not give any insight on the exact mechanism that leads to one morphology or the other.

Torza and Mason [10] proposed that the resulting equilibrium configuration of two immiscible liquid drops suspended in a third immiscible liquid and brought into contact is readily predicted from the interfacial tensions and spreading coefficients. In our system, one of two immiscible liquid drops corresponds to a pure liquid, PFOB, but the other one is a mixture of PLGA and dichloromethane. Moreover, interfacial tensions are in continuous evolution because of dichloromethane evaporation process. To try to interpret the different final capsule morphologies by analyz-

Table 1
Interfacial tensions (mN/m) measured with the pendant drop method

Drop phase	Cuvette phase					
	Water	SC	TC	PVA	CH_2Cl_2	CH_2Cl_2–PLGA
CH_2Cl_2	28.2(±0.1)	8.1(±<0.1)	8.5(±<0.1)	6.6(±0.6)	NA	NA
CH_2Cl_2–PLGA	22.6(±0.3)	7.0(±0.3)	8.3(±0.2)	6.7(±0.3)	NA	NA
CH_2Cl_2–PFOB	27.7(±0.3)	8.2(±<0.1)	8.6(±<0.1)	6.7(±0.4)	NA	NA
CH_2Cl_2–PLGA–PFOB	21.8(±0.4)	6.3(±0.5)	8.1(±0.1)	6.6(±0.2)	NA	NA
PFOB	44.4(±0.4)	15.6(±0.5)	17.5(±0.1)	19.8(±0.4)	4.0(±0.7)	3.5(±0.5)

Note. NA = not applicable. PLGA concentration in CH_2Cl_2 or CH_2Cl_2–PFOB is 25 mg/mL.

Table 2
Initial spreading coefficients (mN/m) calculated from Table 1 results, according to Eq. (1)

	S_1 (PFOB)	S_2 (aqueous surfactant solution)	S_3 (CH_2Cl_2–PLGA)
SC	−12.1	−19.1	5.8
TC	−12.7	−22.3	5.9
PVA	−16.6	−23	9.6

ing the spreading coefficients in the system, interfacial tension measurements have been performed on the (PLGA in CH_2Cl_2)–PFOB–aqueous solution of surfactant system. Since it is impossible to measure interfacial tensions throughout the whole evaporation process, the initial interfacial tensions were measured using the pendant drop method. Results are presented in Table 1. Using these results one can calculate the spreading coefficients, for the three surfactants, as proposed by Torza and Mason (Table 2). Whatever surfactant is used, we obtain values of S_1 and $S_2 < 0$ and of $S_3 > 0$. Therefore, core–shell morphologies should be obtained in the three cases. Experiments are obviously in disagreement with Torza and Mason predictions but one should notice that these spreading coefficients correspond to the initial configuration before dichlormethane evaporation.

However, close examination of interfacial tensions results helps to shed some light on the observed morphologies. Results show that, as expected, PLGA is a poor stabilizer for the dichloromethane–water interface ($\gamma = 23$ mN/m) even in presence of PFOB ($\gamma = 21.8$ mN/m). Moreover, PLGA does not influence the interfacial tension between PFOB and dichloromethane. This strongly suggests that there is not any PLGA adsorbed at the PFOB–dichloromethane interface. One can also notice that PVA is the worst stabilizer of the PFOB–water interface and gives the best stabilization of the dichloromethane–water interface. In addition, the dichloromethane–PVA solution interfacial tension does not vary upon addition of PLGA, confirming that these two polymers do not develop favorable interactions at early times: PVA forms a stable layer at the dichloromethane–water interface that prevents the adsorption of PLGA molecules.

Sodium taurocholate (TC) appears the worst stabilizer of the dichloromethane–water interface. For TC, as observed for PVA, the dichloromethane–TC solution interfacial tension does not vary in the presence of PLGA and PFOB, which proves that the TC layer does not allow other chemical species to adsorb at the interface. In addition TC leads to a greater PFOB–water interfacial tension than SC. Whatever interface is considered, TC surfactant properties are weaker than SC or PVA.

By contrast, with sodium cholate, PLGA and the couple PLGA–PFOB induce a significant decrease of the dichloromethane–water interfacial tension. SC appears as the best stabilizer of the PFOB–water interface. It immediately facilitates the formation of a mixed interfacial layer with PLGA.

While performing interfacial tension measurements, we noticed that in the case of SC and TC, droplets were stable upon time whereas in the case of PVA, droplets were detaching from the needle after about a minute. This confirms the results from Boury et al. [18,19] showing that PVA reorganizes upon time at the dichloromethane–water interface or continues to adsorb. We believe that this reorganization or slow adsorption may allow some PLGA to finally adsorb at the interface and favor the formation of core–shell capsules after evaporation is completed. The final balance between morphologies probably depends on the dynamics of PVA reorganization and PLGA adsorption. Indeed when evaporation is accelerated, the reorganization may not have enough time to fully take place and in the majority of the droplets PLGA cannot adsorb, explaining the increase of the number of acorns.

As a conclusion, just after emulsification, there is a single interface composed of dichloromethane–water stabilized by the surfactant. Since PFOB is very poorly miscible in dichloromethane, the droplet composition reaches quickly the binodal boundary and PFOB phase separates within the emulsion globule of polymer–dichloromethane. Therefore, two interfaces are then present in the system: the aqueous solution–dichloromethane interface and the PFOB–dichloromethane interface. In this system, a good surfactant forms a layer at the dichloromethane–water interface that prevents the contact with PFOB, and PLGA is sandwiched between PFOB and the surfactant layer. On one hand, if PLGA interacts with the surfactant, it reinforces the interfacial layer and finally leads to core–shell capsules as for SC. On the other hand, if the surfactant prevents the adsorption of other substances, water can come in contact with PFOB and because of water and PFOB poor affinity ($\gamma = 44.4$ mN/m), they phase separate developing “acorns” morphologies as for TC. Since PVA reorganizes at the interface, for some droplets, PLGA cannot adsorb whereas for others it may finally adsorb at the interface explaining the coexistence of the two morphologies. The exact conformation of SC and TC at the water–dichloromethane interface should be studied in the future to explain why surfactants with such a similar chemical structure have a different interfacial behavior.

4. Conclusion

We have studied the influence of three surfactants on the encapsulation of PFOB within PLGA capsules. On one hand, when sodium taurocholate is used, one can observe acorn morphologies in which a hemisphere of liquid PFOB coexists with a hemisphere of solid PLGA. On the other hand, when sodium cholate is used, liquid PFOB is perfectly encapsulated within a solid PLGA shell. The behavior with PVA is in between the two other cases with coexistence of acorns and core–shell capsules in a same suspension. None of the formulation parameters such as the evaporation speed or the PLGA concentration allows to totally displace the equilibrium towards one morphology or another. Microscopic observations of morphologies development during the evaporation process show that the position of the PFOB droplet in the emulsion globules after one hour of evaporation might help predicting the final morphology. Experimental determination of the spreading coefficients demonstrates that Torza and Mason theory fails to correctly predict the observed morphology of polymer–liquid colloids because they consider equilibrium configurations and neither dynamic effects nor the detail of the interfacial organization have been taken into account. Close examination of the interfacial

tension values measured at the three interfaces allows proposing a hypothesis explaining the differences in capsule morphologies. There is a competition between PLGA and the surfactant stabilizing the emulsion at the water–dichloromethane interface, if PLGA is able to adsorb, the core–shell morphology is obtained, otherwise the acorn morphology is observed. When the surfactant rearranges at the interface upon time, a coexistence of morphologies can be observed.

Acknowledgments

Authors acknowledge financial support from Agence Nationale de la Recherche (ANR ACUVA NT05-3_42548) in particular for E. Pisani fellowship. Authors would like to thank D. Jaillard and J. Degrouard (CCME, Orsay) for TEM experiments, A. Allavena-Valette (CECM, Vitry^{S}/Seine) for access to the SEM facility and V. Nicolas for help with confocal microscopy (IFR 141-ITFM, Châtenay-Malabry).

References

[1] R. Gramiak, P.M. Shah, Invest. Radiol. 3 (1968) 356.
[2] J.M. Correas, S.L. Bridal, A. Lesavre, A. Mejean, M. Claudon, O. Helenon, Eur. Radiol. 11 (2001) 1316.
[3] A.M. Reed, D.K. Gilding, Polymer 22 (1981) 494.
[4] K. Yamaguchi, J.M. Anderson, J. Controlled Release 24 (1993) 81.
[5] E. Pisani, N. Tsapis, J. Paris, V. Nicolas, L. Cattel, E. Fattal, Langmuir 22 (2006) 4397.
[6] E. Pisani, N. Tsapis, B. Galaz, M. Santin, R. Berti, N. Taulier, E. Kurtisovski, O. Lucidarme, M. Ourevitch, B.T. Doan, J.C. Beloeil, B. Gillet, W. Urbach, S.L. Bridal, E. Fattal, Adv. Funct. Mater. (2008), in press.
[7] M. Andre, T. Nelson, R. Mattrey, Invest. Radiol. 25 (1990) 983.
[8] D.C. Sundberg, P.A. Casassa, J. Pantazopoulos, M.R. Muscato, B. Kronberg, J. Berg, J. Appl. Polym. Sci. 41 (1990) 1425.
[9] F.M. Lavergne, D. Cot, F. Ganachaud, Langmuir 23 (2007) 6744.
[10] S. Torza, S.G. Mason, J. Colloid Interface Sci. 33 (1970) 67.
[11] J. Berg, D.C. Sundberg, B. Kronberg, J. Microencapsulation 6 (1989) 327.
[12] W. Abdelwahed, G. Degobert, H. Fessi, Int. J. Pharm. 309 (2006) 178.
[13] A. Loxley, B. Vincent, J. Colloid Interface Sci. 208 (1998) 49.
[14] P.J. Watts, M.C. Davies, C.D. Melia, Crit. Rev. Ther. Drug Carrier Syst. 7 (1990) 235.
[15] R. Arshady, J. Controlled Release 17 (1991) 1.
[16] M. Audran, M.P. Krafft, J. De Ceaurriz, J.C. Mathurin, M.T. Sicart, B. Marion, F. Fabre, F. Bressolle, J. Chromatogr. B Biomed. Sci. Appl. 734 (1999) 267.
[17] D.R. Lide, CRC Handbook of Chemistry and Physics, 82nd rev. ed., 2001, p. 2664.
[18] F. Boury, E. Olivier, J.E. Proust, J.P. Benoit, J. Colloid Interface Sci. 163 (1994) 37.
[19] F. Boury, T. Ivanova, I. Panaïotov, J.E. Proust, A. Bois, J. Richou, J. Colloid Interface Sci. 169 (1995) 380.